npj | regenerative medicine

Article

Published in partnership with the Australian Regenerative Medicine Institute

https://doi.org/10.1038/s41536-025-00432-z

Exosome injection as a prevention strategy for early postoperative mesh complications in a porcine model of sacrocolpopexy

Cassandra K. Kisby[1] ✉, Sam Faraguna[2], Abigail Hitt[3], Ilya Y. Shadrin[4], Hunter Newman[5,6], Anna Gilpin[5,6], Cindy L. Amundsen[1] & Shyni Varghese[5,6]

Exosomes, an acellular regenerative biologic, have demonstrated success in *resolving* vaginal mesh exposures after pelvic reconstructive surgery; little data exists for their use for *prevention* of mesh-based complications. This study evaluated the early efficacy of purified exosome product (PEP) for preventing mesh exposures. Ten Yorkshire-crossed pigs underwent mesh sacrocolpopexy with two high-risk-for-exposure configurations: mesh fold ventrally, vaginotomy dorsally. PEP in hyaluronic acid (HA) or HA-only (control) was injected at baseline. Twelve weeks later, animals were euthanized and evaluated for mesh exposure and histologic changes. None of the PEP-treated tissues demonstrated mesh exposure (0/6); all control group animals experienced a mesh exposure (4/4 mesh fold configuration, 2/4 vaginotomy configuration). Control tissues exhibited higher fibrosis (vaginotomy fibrosis score: median(IQR); 3(3,3) control, 2(1,2) PEP; $p = 0.03$) and greater epithelial apoptosis (mesh fold TUNEL+area fraction: median 18.9 control vs 0.43 PEP; $p = 0.02$). Our study demonstrated that PEP treatment mitigated the risk of early mesh exposure.

Surgical implantation of polypropylene mesh during sacrocolpopexy is an accepted and durable treatment for women experiencing pelvic organ prolapse, but carries a risk of vaginal mesh exposure, which is often treated via mesh excision[1–3]. Rates of mesh exposure following mesh sacrocolpopexy range from 1 to 10%, and reoperation for mesh-based complications range from 8 to 40%[4–12]. Two potential strategies for reducing mesh-based complications are to modify mesh properties or modulate the host's tissue environment and regenerative efforts. Our study focuses on the latter.

Regenerative medicine technologies have received increasing attention in Gynecology and Urogynecology. Examples of such applications include endometrial optimization for fertility indications and muscle and connective tissue regeneration for pelvic floor disorders[13,14]. Exosomes, a type of extracellular vesicle that can be harvested from various tissues and cells, including bone marrow, plasma, and urine, have been utilized as an acellular regenerative technology. Exosomes' mechanism of action is purported to be multifactorial, including inciting host regeneration through activation of autocrine and paracrine pathways. Exosomes have been purified and made available as a clinical-grade product, purified exosome product (PEP; Rion LLC; Rochester, Minnesota). This product is manufactured into a shelf-stable lyophilized powder from pooled human plasma; thus, the exosomes are of platelet origin. PEP has shown regenerative capacity for bone, muscle, and connective tissue in preclinical and clinical studies[15–20]. In our pilot studies using a porcine model, injection of PEP induced tissue regeneration and *resolved* vaginal mesh exposures following mesh-augmented pelvic reconstructive surgeries[21,22].

In this study we aim to evaluate the efficacy of PEP for early *prevention* of vaginal mesh exposure in high-risk sacrocolpopexy mesh configurations and examine changes to the local tissue. We hypothesize that mesh-vagina complexes injected with PEP would experience fewer mesh exposures in the early post operative period, as compared to control, and demonstrate more favorable histologic characteristics.

[1]Duke Health, Department of Obstetrics and Gynecology, Division of Urogynecology, Durham, NC, USA. [2]Duke University, Durham, NC, USA. [3]Duke Health, Department of Pathology, Durham, NC, USA. [4]Duke Health, Department of Medicine, Division of Cardiology, Durham, NC, USA. [5]Duke Health, Department of Orthopedics, Durham, NC, USA. [6]Duke University, Department of Biomedical Engineering, Mechanical Engineering and Materials Sciences, Durham, NC, USA. ✉e-mail: Cassandra.kisby@duke.edu

Results

All animals tolerated the procedures without clinically significant adverse events. Of note, a formal cadaveric and histologic safety assessment was not performed due to demonstration of safety of the test article in prior studies.

All animals in the control group ($n = 4$) demonstrated mesh exposures on gross examination. In the control group, there were two non-significant exposures (<1 cm; exposures overlying the prior vaginotomy) with the vaginotomy mesh configuration and one non-significant (2 cm caudal to the center-most portion of the mesh fold) and three significant exposures (≥1 cm; exposures overlying the central twisted portion of the mesh fold) with the mesh fold configuration. No animals in the PEP group ($n = 6$) demonstrated a mesh exposure. Gross examples of presence and absence of mesh exposure are demonstrated in Fig. 1.

In the control group, both the mesh fold and vaginotomy conditions, evaluation of H&E and trichrome-stained sections revealed contracture or loss of spacing of mesh fibers, creating mesh aggregates with a greater number of mesh fibers in cross-section on histology. These control group aggregates were subjectively noted to contain peri-mesh edema, fibrosis, and inflammatory cells (Fig. 2a). In the control group with the mesh fold, the vaginal epithelium demonstrated disruption of the epithelial architecture and was more discontinuous, which is consistent with the presence of gross mesh exposures (Fig. 2b). Comparison of histologic scoring between treatment groups for the vaginotomy mesh configuration showed a significant difference in fibrosis (median (IQR); 3(3,3) control, 2(1,2) PEP; $p = 0.03$). There were no significant differences between treatment groups, in either mesh condition, for inflammation or neovascularization (Fig. 3a, b).

For peri-mesh apoptosis, there were more samples in the control group, which demonstrated high TUNEL+ signal around mesh fibers, but the variance across specimens resulted in a statistically non-significant difference (Fig. 4a). For epithelial apoptosis, the mesh fold condition demonstrated more apoptosis in the control group as compared to the PEP-treated group (Fig. 4b; median 18.9 vs 0.43; $p = 0.02$).

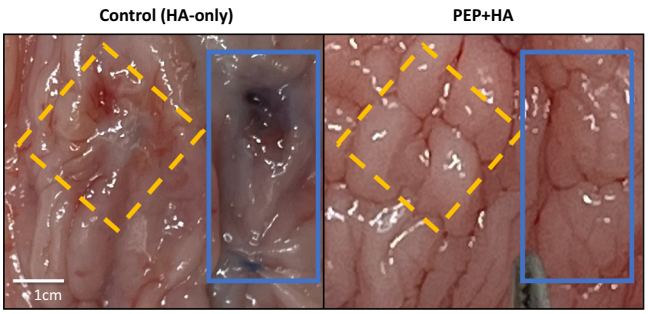

Fig. 1 | Photographs comparing gross appearance by group (Control vs PEP + HA) and condition (mesh fold vs vaginotomy): Note - the vaginas were detubularized to allow photography of both mesh conditions side-by-side. The locations of the vaginotomy are marked with dashed-line yellow diamonds, the folded mesh by solid-line blue rectangles. The control tissues demonstrated thinner tissue over the mesh and vaginal mesh exposures, which were more common in the mesh fold condition. The mesh used in the experiments is blue, which is evident in the Control mesh exposure (left).

Discussion

In this preclinical large animal study using an injectable exosome regenerative therapy in an at-risk for exposure mesh sacrocolpopexy model, exosome delivery using an HA carrier was found to decrease the incidence of early vaginal mesh exposures, as compared to control groups administered with HA-only. In fact, mesh exposures were only found in the control tissues, and none were present in the exosome-treated tissues. We evaluated two at-risk for exposure mesh configurations in each animal—vaginotomy and mesh fold—and the mesh fold configuration more frequently experienced a delayed mesh exposure, making it the more at-risk configuration of the two evaluated. In addition to differences in gross mesh exposure incidence, on the tissue level, we found lower fibrosis and apoptosis in exosome-treated groups as compared to control tissues, suggesting a more favorable tissue-level environment.

It is important to note that even in the setting of estrogen deprivation and high-risk mesh configurations, the exosome group still experienced prevention of mesh exposures at the 12-week endpoint. While the role of estrogen in immediate regeneration is not completely characterized, it is thought to be detrimental to the first phase of macrophage infiltration and potentially macrophage phenotype switching, which can lead to a fibrotic rather than regenerative environment; however, from a clinical standpoint, the absence of estrogen also leads to vaginal tissue thinning, which increases the risk of mesh exposure[9,23,24]. In fact, vaginal estrogen cream is often utilized as a first-line treatment for vaginal mesh exposure. In summary, the role of estrogen may both be positive and negative depending on the timing of exposure; however, the postmenopausal state is generally considered to increase the long-term risk of mesh exposure. Our goal was to create a highly at-risk for exposure model; thus, we chose to perform an oophorectomy and still demonstrated differences in tissue regeneration and a difference in mesh exposure prevention between groups.

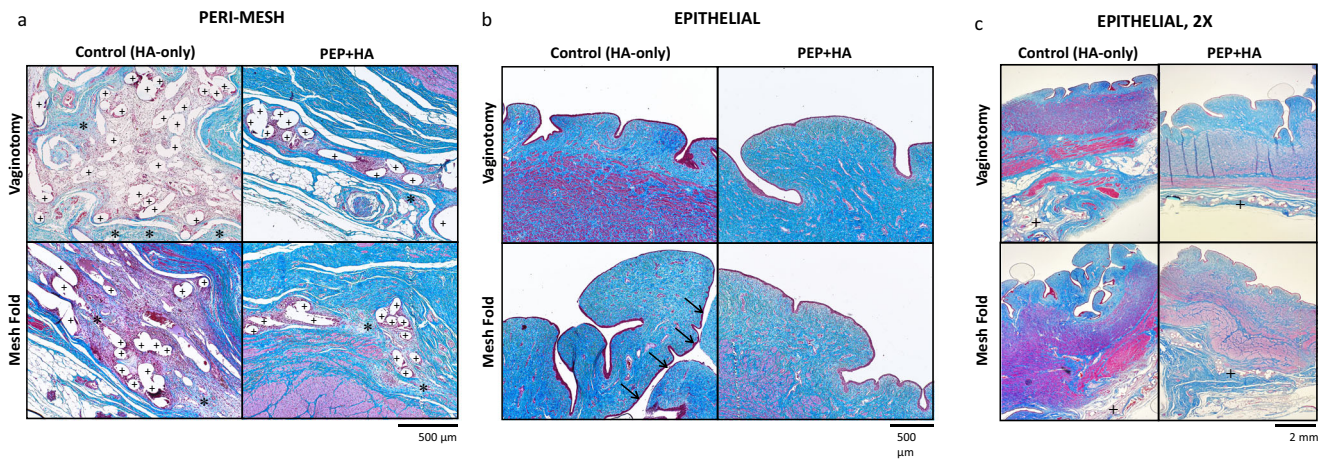

Fig. 2 | Epithelial and Peri-Mesh Histology by Group and Condition. **a** Microscopic photographs demonstrating greater peri-mesh reactive edema with associated fibrosis (denoted by *) in control tissues compared to PEP + HA. For identification, mesh fibers are denoted by "+"; **b**, **c**) Microscopic photographs at 10X (**b**) and 2X (**c**) demonstrating differences in epithelial architecture between control and PEP + HA tissues, notably epithelial architecture disruption (denoted by arrows, **b** in the control tissues with a mesh fold. Masson's Trichrome stain.

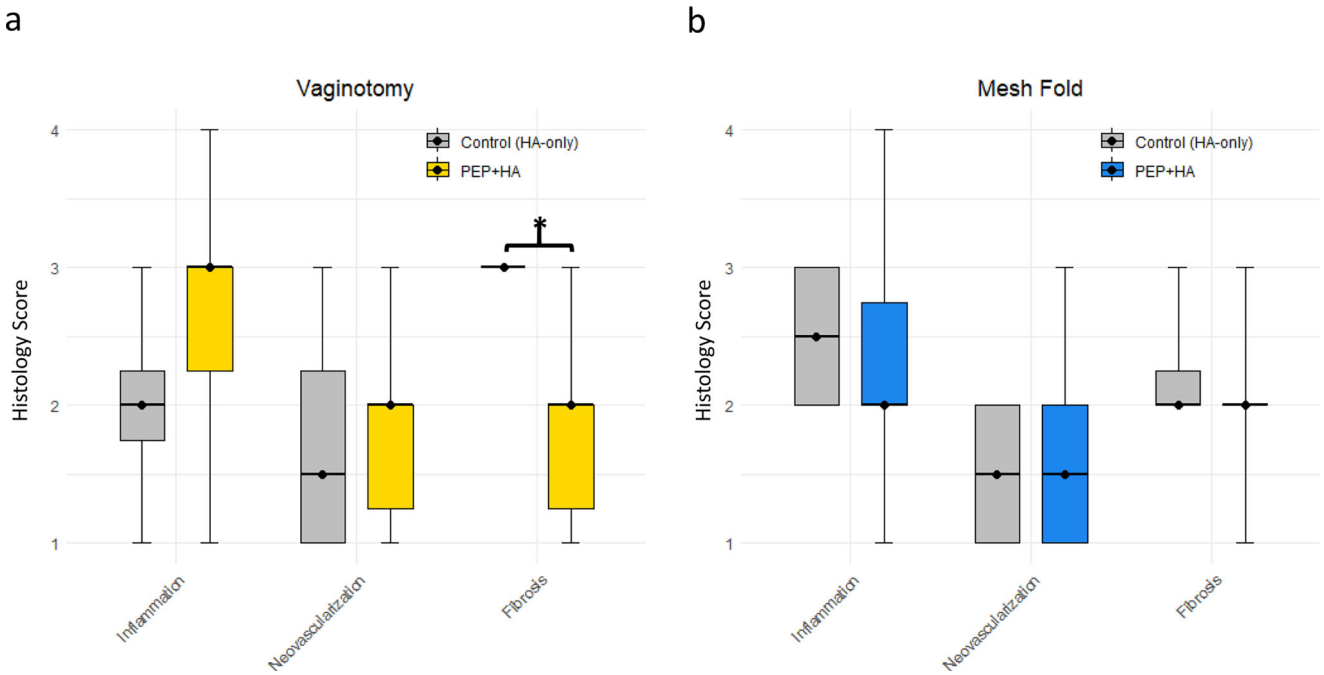

Fig. 3 | Histologic Scoring outcomes comparing Control and PEP+HA outcomes by mesh configuration (Vaginotomy or Mesh Fold). a With the vaginotomy mesh configuration, perimesh inflammation and neovascularization were not statistically different between Control and PEP+HA groups. There was significantly less fibrosis ($P < 0.05$) in the PEP+HA tissues as compared to the Control tissues. **b** There were no statistically significant differences in histology scores between treatment conditions with the mesh fold configuration.

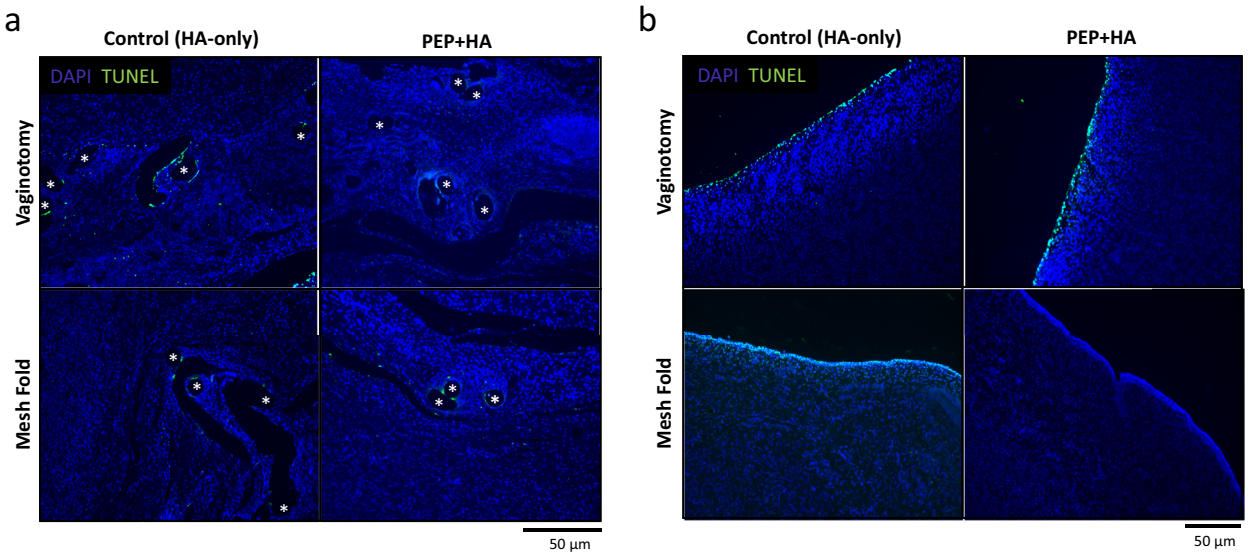

Fig. 4 | Microscopic photographs using Thermo Fisher Click-iT TUNEL staining (TUNEL staining is green; Dapi staining for nuclei is blue). a There is greater perimesh apoptosis in control tissues compared to PEP + HA for the vaginotomy condition, but this is nonsignificant by mesh condition. Mesh fibers are denoted by *. **b** There is greater apoptosis in all layers of the control epithelial tissues as compared to PEP + HA tissues; apoptosis in the mesh fold condition is significantly higher in the control group ($p = 0.02$).

Many studies have demonstrated the deleterious effects of certain mesh materials (i.e. polypropylene) and configurations[25–29]. While new mesh materials are not yet available for clinical practice, factors surgeons have control over largely surround choice of mesh with certain characteristics (e.g., volume of mesh, weave, pore collapse, pore size, weight) and surgical technique[1,30,31]. In our study, we utilized a lightweight polypropylene mesh with large pores and relatively low pore collapse, given its common use in our specialty, Urogynecology. The intent was to also minimize the contribution of the mesh itself to regeneration or lack-of. One of the two high-risk configurations used was extrapolated from a model demonstrated in New Zealand white rabbits by Knight et al. showing mesh implants with folds were more likely to be associated with mesh exposures[25]. This makes sense, as a fold or buckle in the mesh creates focal points of mechanical stress and pore collapse, both of which have been shown to increase the risk of mesh exposure[32]. In our study, we also saw higher apoptosis in the area of the mesh fold in the control tissues. In clinical practice, surgeons may experience the dilemma of whether to place a mesh implant if an incidental vaginotomy is made. We replicated this in our model. Both mesh configurations were evaluated, with the mesh fold being the worst of the configurations and leading to more mesh exposures. Exosome injection did

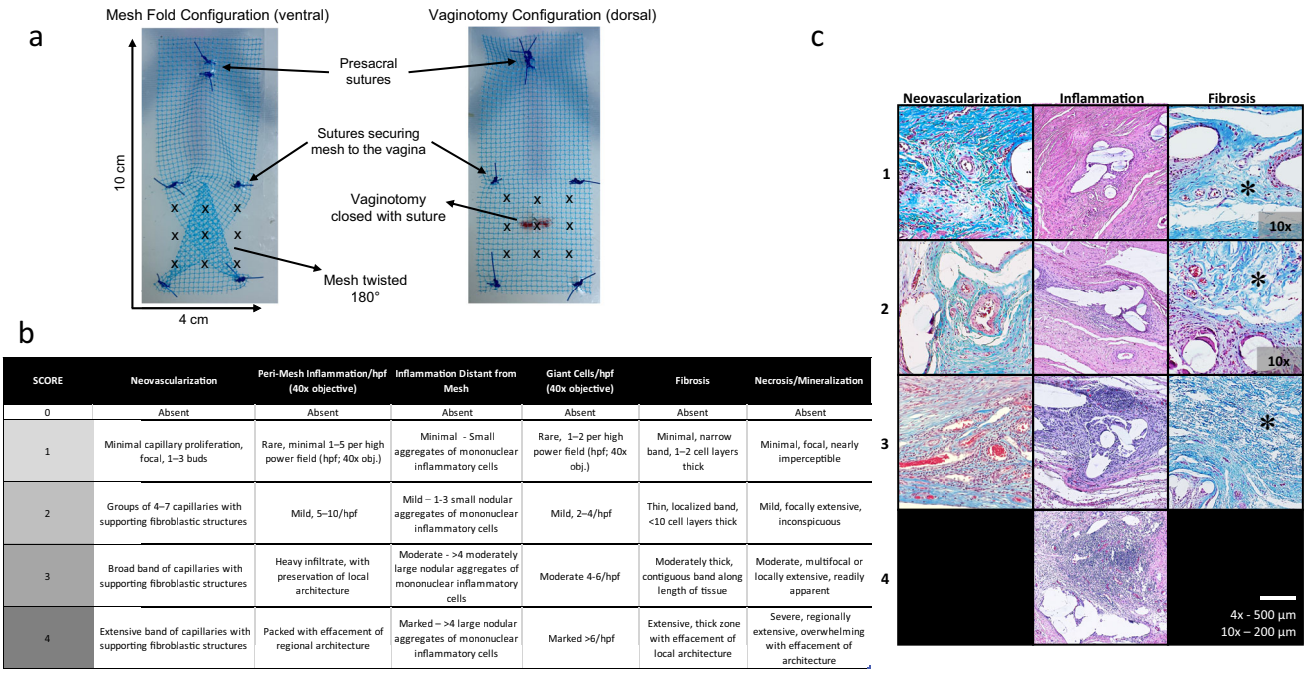

SCORE	Neovascularization	Peri-Mesh Inflammation/hpf (40x objective)	Inflammation Distant from Mesh	Giant Cells/hpf (40x objective)	Fibrosis	Necrosis/Mineralization
0	Absent	Absent	Absent	Absent	Absent	Absent
1	Minimal capillary proliferation, focal, 1–3 buds	Rare, minimal 1–5 per high power field (hpf; 40x obj.)	Minimal - Small aggregates of mononuclear inflammatory cells	Rare, 1–2 per high power field (hpf; 40x obj.)	Minimal, narrow band, 1–2 cell layers thick	Minimal, focal, nearly imperceptible
2	Groups of 4–7 capillaries with supporting fibroblastic structures	Mild, 5–10/hpf	Mild – 1-3 small nodular aggregates of mononuclear inflammatory cells	Mild, 2–4/hpf	Thin, localized band, <10 cell layers thick	Mild, focally extensive, inconspicuous
3	Broad band of capillaries with supporting fibroblastic structures	Heavy infiltrate, with preservation of local architecture	Moderate - >4 moderately large nodular aggregates of mononuclear inflammatory cells	Moderate 4-6/hpf	Moderately thick, contiguous band along length of tissue	Moderate, multifocal or locally extensive, readily apparent
4	Extensive band of capillaries with supporting fibroblastic structures	Packed with effacement of regional architecture	Marked – >4 large nodular aggregates of mononuclear inflammatory cells	Marked >6/hpf	Extensive, thick zone with effacement of local architecture	Severe, regionally extensive, overwhelming with effacement of architecture

Fig. 5 | Methods. a high risk mesh implantation configurations: left represents mesh implanted with a fold, right represents mesh implanted over a vaginotomy; mesh is attached with interrupted sutures of 2-0 polypropylene (blue) and the vaginotomy is closed with 2-0 polyglactin 910; the 3 × 3 injection pattern of HA or PEP + HA is marked with X's; **b** Histology scoring system; **c** Microscopic photographs displaying sample scoring of neovascularization, peri-mesh inflammation, and fibrosis (denoted with an asterisk) using the Histology scoring system. Masson's Trichrome and Hematoxylin & Eosin staining are depicted. There are no representative histologic images for a score of 4 for both neovascularization and fibrosis (represented as a black boxes in **c**. All micrographs were taken with a 4x objective unless otherwise noted in the figure.

mitigate this, as exosome-treated tissues in our study did not experience exposures in the early postoperative period. In the absence of exosome therapy, surgeons should take caution to prevent mesh folds and buckles, though these are sometimes inevitable in a contracted pelvis, multi-operated vagina, or with individual anatomic differences. Should regenerative technologies become mainstream, these technologies, such as exosomes, may be able to mitigate the risk of mesh exposure when a mesh fold or buckle is unavoidable or a vaginotomy has occurred.

Our study had several limitations, some of which are inherent to large animal preclinical studies and others due to the use of a porcine model. Our sample size was, overall, modest; however, the data acquired were maximized by creating two mesh conditions in each animal. Due to our modest sample size, we may not achieve statistical significance for some outcomes due to insufficient power. Use of a large animal model is advantageous for clinical outcomes; however, histological analysis, specifically immunohistochemistry, is challenging in pig tissues. We had intended to characterize the immune response and demonstrate fibrosis via immunohistochemistry, but the antibodies were not reliable in the study tissues. We, instead, relied on histologic scoring from a blinded histopathologist. Lastly, while 12 weeks is a significant time period for a preclinical large animal study, it is still considered a short-term follow-up in the clinical realm and it is unknown if the positive effects of the exosomes on the tissues will dissipate with time.

The strengths of our study include the use of a large animal model with anatomy that is similar to human vaginal anatomy and allowed for implantation of a clinically meaningful-sized mesh implant. We carried out our study to 12 weeks, which would capture the chronicity of wound remodeling and fibrosis, as well as contracture, which can occur with implantation of polypropylene mesh. The mesh was also implanted and tensioned, as it would be in human surgery, to semi-replicate the biomechanical forces the mesh-vagina complex would normally experience – the authors recognize the quadrupedal nature of porcine ambulation, rather than bipedal in human primates. We used a regenerative product, PEP, that is manufactured via an automated process and is shelf-stable. These characteristics make the regenerative biologic easy to use and the treatment easy to replicate, a major advantage over cell transplantation-based therapeutics. Lastly, we completed a universal oophorectomy to create a postmenopausal-like state to mimic the thinner vaginal tissues in postmenopausal women.

The results of this preclinical porcine study evaluating early postoperative mesh exposure *prevention* in an at-risk for mesh exposure sacrocolpopexy model suggest that regenerative technologies, such as exosomes, may improve the tissue-level environment and regeneration, leading to prevention of vaginal mesh exposures. The current study represents a modest sample and endpoint; further study should evaluate the mitigation of mesh exposure risk in a larger sample and persistence of the test article's effect by using a longer end point.

Methods

All procedures were approved by the Institutional Animal Care and Use Committee (Protocol 22–264). The at-risk for exposure model was extrapolated from a model created in rabbits and general surgical principles from clinical experience[25].

Experimental design

Ten Yorkshire-Crossed pigs (50–60 Kg) underwent survival surgeries at baseline to create an at-risk for vaginal mesh exposure model. The model was created by first performing an open abdominal hysterectomy and oophorectomy; a ventral and dorsal vaginal dissection were then performed per typical fashion for a sacrocolpopexy. Type I polypropylene mesh (Vertessa Lite, Caldera Medical, Westlake Village, CA) was applied in two at-risk configurations in all animals ($n = 10$): 1) a mesh buckle (i.e., twisted mesh) ventrally, and 2) 1 cm vaginotomy repaired with an interrupted

polyglactin 910 suture and mesh applied overtop dorsally (Fig. 5a). Mesh implants were 4 x 10 cm in size. The proximal arm of thesh was attached to the sacrum with 2-0 polypropylene suture, tensioned such that the vagina was elevated 2 cm from its position at rest. Animals were randomized to receive a PEP injection ($n = 6$) or control injection ($n = 4$) at the time of sacrocolpopexy; the ventral and dorsal mesh conditions were treated with the same test article per animal.

Injection of purified exosome product (PEP) or hyaluronic acid (control)

A working solution of 20% PEP was created by reconstituting 5 x 10^{12} lyophilized exosomes (PEP; Rion LLC, Rochester, MN) in 1 mL of sterile water (Hospira Inc., Lake Forest, IL) and then mixing with 4 mL of clinical-grade hyaluronic acid (HA) (12 mg/mL; Lifecore Biomedical, Chaska, MN). A total of 5 mL of PEP mixture was injected by a masked surgeon, split between the ventral and dorsal vagina. The hydrogel was injected into the fibromuscular tissue under each mesh implant, evenly across nine sites (in a 3 × 3 grid pattern, Fig. 5a) using a 22-gauge needle.

Animals in the control group received injections of 4 mL of hyaluronic acid, split between the ventral and dorsal vagina, in a 3 × 3 injection grid pattern. Note that the injected volume is 1 mL less for the control group than the PEP + HA group given sterile water was needed to reconstitute the exosomes in the PEP + HA group.

Tissue harvest and histologic processing

Twelve weeks following the baseline injections, all animals were euthanized using pentobarbital. Genitourinary organs were excised en-bloc, detubularized to allow them to lay flat, and photographed. Subsequently, the center-most portion of vagina-mesh complexes was sampled using a scalpel, placed into cassettes and immersed in formalin. Formalin-fixed paraffin-embedded tissues were sectioned at 10 µm on a microtome. Sections were processed for Hematoxylin and Eosin (H&E) and Masson's Trichrome (trichrome) staining according to standard lab protocols.

To evaluate tissue apoptosis, we utilized a TUNEL assay, which inserts a labeled nucleotide on the 3'-OH end of damaged DNA. For the assay, samples were incubated in 4% paraformaldehyde for 15 min at 37 °C. The slides were then placed in a 0.25% Triton X-100 PBS mixture and incubated for 15 min. Using the Click-iT Plus TUNEL Assay (Thermo Fisher; C10617) and corresponding procedure, the TdT reaction and Click-iT Plus reaction were performed. During the Click-iT Plus reaction, Alexa Fluor® 488 picolyl azide (Invitrogen) secondary antibodies were diluted to 1:1000 and incubated for 30 min at 37 °C. Following washes, Invitrogen ProLong Gold Antifade Mountant with DAPI® was used to seal coverslips on each slide. Sections were imaged using a 4x, 10x and 20x objectives on a Motic Easy Scan Pro Digital Slide Scanner.

Quantification and statistical analysis

Mesh exposure quantification. Mesh-vagina complexes were detubularized and evaluated for presence or absence of a mesh exposure. Mesh exposure was defined as mesh fibers protruding through the full thickness of the epithelium and into the vaginal lumen. Dimensions of the mesh exposure were obtained using a photo processing program and confirmed based on measurement via calipers on fresh tissues. Exposures were categorized as non-significant (<0.5 cm) or significant (≥1 cm) based on size, with the significance threshold being determined by clinical experience.

Histologic quantification. Histologic analysis was performed by a blinded Pathologist. The investigator assigned a numerical score (0–4) for inflammation near the region of interest (ROI), inflammation distant from the ROI, giant cells, neovascularization, fibrosis, necrosis, and mineralization (Fig. 5b). Representative images of histological scoring are demonstrated in Fig. 5c. Scores for PEP versus control groups were compared.

TUNEL quantification. Images were analyzed using a custom, semi-automated macro in FIJI (ImageJ, version 1.54 f, National Institutes of Health). Briefly, 10x magnification overlay images containing DAPI and TUNEL signal were input into ImageJ. For epithelial TUNEL analysis, regions of epithelium were manually traced (epithelial ROI) based on increased DAPI density and epithelial appearance at tissue edges. Epithelial ROI were overlaid with TUNEL images, and semi-automated thresholding was adjusted to exclude background fluorescence. TUNEL positivity was reported as TUNEL+ area fraction for each ROI, defined as TUNEL + area divided by total area of ROI (dimensionless). For deeper tissue areas with mesh, total mesh fiber area (voids from individual mesh fibers) was manually traced and calculated. Subsequently, a larger ROI surrounding the mesh area extending circumferentially roughly 80–100 um (the diameter of a single mesh fiber) around mesh fibers was manually drawn, and total mesh fiber area was subtracted to yield net peri-mesh fiber tissue area (peri-mesh ROI). TUNEL images were overlaid onto the peri-mesh ROI, from which TUNEL+ area fraction of the peri-mesh ROI was calculated as above. In all analyses, areas of obvious artifact were excluded.

JMP Pro (Version 8, Cary, NC) was used for statistical analysis. Data were reported as median (inter-quartile range (IQR)), number (percents), and counts as appropriate for the outcome. Where appropriate, data were analyzed with non-parametric tests, Kruskal-Wallis and Mann-Whitney tests with a Bonferroni correction. For data with non-numerical comparisons, data visualization techniques were used. A significance level was set to α of 0.05.

Data availability

The datasets generated and/or analyzed during the current study are available from the corresponding author on reasonable request.

Received: 10 September 2024; Accepted: 26 August 2025;
Published online: 29 September 2025

References

1. Developed by the Joint Writing Group of the American Urogynecologic Society & the International Urogynecological Association & affirmed by the American Association of Gynecologic Laparoscopists, the Society of Gynecologic Surgeons Joint position statement on the management of mesh-related complications for the FPMRS specialist. *Female Pelvic Med Reconstr. Surg*. **26**, 219–232 (2020).
2. Committee Opinion No. 694: management of mesh and graft complications in gynecologic surgery. *Obstet Gynecol.* **129**, e102–e108, https://doi.org/10.1097/AOG.0000000000002022 (2017).
3. Addison, W. A., Cundiff, G. W., Bump, R. C. & Harris, R. L. Sacral colpopexy is the preferred treatment for vaginal vault prolapse. *J. Gynecol. Tech*. **2**, 69–74 (1996).
4. Stepanian, A. A., Miklos, J. R., Moore, R. D. & Mattox, T. F. Risk of mesh extrusion and other mesh-related complications after laparoscopic sacral colpopexy with or without concurrent laparoscopic-assisted vaginal hysterectomy: experience of 402 patients. *J. Minim. Invasive Gynecol.* **15**, 188–196 (2008).
5. Thomas, T. N., Davidson, E. R. W., Lampert, E. J., Paraiso, M. F. R. & Ferrando, C. A. Long-term pelvic organ prolapse recurrence and mesh exposure following sacrocolpopexy. *Int Urogynecol. J.* https://doi.org/10.1007/s00192-020-04291-8 (2020).
6. Chughtai, B. et al. Long-term device outcomes of mesh implants in pelvic organ prolapse repairs. *Obstet. Gynecol.* **135**, 591–598 (2020).
7. Wong, K. S. et al. Adverse events associated with pelvic organ prolapse surgeries that use implants. *Obstet. Gynecol.* **122**, 1239–1245 (2013).
8. Matthews, C. A. et al. Long-term mesh exposure after minimally invasive total hysterectomy and sacrocolpopexy. *Int Urogynecol. J.* **34**, 291–296 (2023).

9. Kisby, C. K. & Linder, B. J. Management of vaginal mesh exposures following female pelvic reconstructive surgery. *Curr. Urol. Rep.* **21**, 57 (2020).
10. Warembourg, S., Labaki, M., de Tayrac, R., Costa, P. & Fatton, B. Reoperations for mesh-related complications after pelvic organ prolapse repair: 8-year experience at a tertiary referral center. *Int. Urogynecol. J.* **28**, 1139–1151 (2017).
11. van Zanten, F. et al. Long-term mesh erosion rate following abdominal robotic reconstructive pelvic floor surgery: a prospective study and overview of the literature. *Int. Urogynecol. J.* https://doi.org/10.1007/s00192-019-03990-1 (2019).
12. van Zanten, F. et al. Mesh exposure after robot-assisted laparoscopic pelvic floor surgery: a prospective cohort study. *J. Minim. Invasive Gynecol.* **26**, 636–642 (2019).
13. Henderson, T., Christman, K. L. & Alperin, M. Regenerative medicine in urogynecology: where we are and where we want to be. *Urogynecology* **30**, 519–527 (2024).
14. Balough, J. L. & Moalli, P. Regenerative medicine in gynecology. *Obstet. Gynecol.* **143**, 767–773 (2024).
15. Rolland, T. J. et al. Exosome biopotentiated hydrogel restores damaged skeletal muscle in a porcine model of stress urinary incontinence. *npj Regen. Med.* **7**, 58 (2022).
16. Shi, G. et al. A novel engineered purified exosome product patch for tendon healing: an explant in an ex vivo model. *J. Orthop. Res.* https://doi.org/10.1002/jor.24859 (2020).
17. Qi, J. et al. Cellular effects of purified exosome product on tenogenesis. *J. Orthop. Res.* https://doi.org/10.1002/jor.24587 (2020).
18. Mazzucchelli, L. et al. A Ready-to-Use Purified Exosome Product for Volumetric Muscle Loss and Functional Recovery. *Tissue Eng. Part A* **29**, 481–490 (2023).
19. Wan, R., Hussain, A., Behfar, A., Moran, S. L. & Zhao, C. The therapeutic potential of exosomes in soft tissue repair and regeneration. *Int. J. Mol. Sci.* **23**, https://doi.org/10.3390/ijms23073869 (2022).
20. Miller, C. M. et al. Platelet-derived exosomes induce cell proliferation and wound healing in human endometrial cells. *Regen. Med.* **17**, 805–817 (2022).
21. Kisby, C. K. et al. Exosome-induced vaginal epithelial regeneration in a porcine mesh exposure model. *Female Pelvic Med. Reconstruc. Surg.* **25**, S111–112 (2019).
22. Kisby, C. K. et al. Impact of repeat dosing and mesh exposure chronicity on exosome-induced vaginal tissue regeneration in a porcine mesh exposure model. *Female Pelvic Med. Reconstr. Surg.* **27**, 195–201 (2021).
23. Zambon, J. P. & Badlani, G. H. Vaginal mesh exposure presentation, evaluation, and management. *Curr. Urol. Rep.* **17**, 65 (2016).
24. Linder, B. J., El-Nashar, S. A., Carranza Leon, D. A. & Trabuco, E. C. Predictors of vaginal mesh exposure after midurethral sling placement: a case-control study. *Int. Urogynecol. J.* **27**, 1321–1326 (2016).
25. Knight, K. M. et al. New Zealand white rabbit: a novel model for prolapse mesh implantation via a lumbar colpopexy. *Int. Urogynecol. J.* **31**, 91–99 (2020).
26. Jallah, Z. et al. The impact of prolapse mesh on vaginal smooth muscle structure and function. *BJOG* **123**, 1076–1085 (2016).
27. Brown, B. N. et al. Characterization of the host inflammatory response following implantation of prolapse mesh in rhesus macaque. *Am. J. Obstet. Gynecol.* **213**, 668 e661–610 (2015).
28. Feola, A. et al. Deterioration in biomechanical properties of the vagina following implantation of a high-stiffness prolapse mesh. *BJOG* **120**, 224–232 (2013).
29. Knight, K. M. et al. A soft elastomer alternative to polypropylene for pelvic organ prolapse repair: a preliminary study. *Int. Urogynecol. J.* **33**, 327–335 (2022).
30. Chughtai, B. et al. Association between the amount of vaginal mesh used with mesh erosions and repeated surgery after repairing pelvic organ prolapse and stress urinary incontinence. *JAMA Surg.* **152**, 257–263 (2017).
31. Dykes, N., Karmakar, D. & Hayward, L. Lightweight transvaginal mesh is associated with lower mesh exposure rates than heavyweight mesh. *Int. Urogynecol. J.* https://doi.org/10.1007/s00192-020-04270-z (2020).
32. Knight, K. M. et al. Mesh deformation: a mechanism underlying polypropylene prolapse mesh complications in vivo. *Acta Biomater.* **148**, 323–335 (2022).

Acknowledgements

This work was supported by the K12 Urologic Research (KURe) Grant (K12DK100024) and the AHA-Doris Duke Foundation (2021274-OF). The funding agencies played no role in study design, data collection, analysis and interpretation of data, or writing of this manuscript.

Author contributions

C.K.: study design, surgeries, data analysis, and manuscript preparation; S.F.: surgeries and data analysis; A.H.: histology, data analysis, and manuscript preparation; I.S.: data analysis and manuscript preparation; H.N.: histology; A.G.: histology; C.A.: study design and manuscript preparation; S.V.: study design, lab resources, and manuscript preparation.

Competing interests

C.K. has a filed patent for a vaginal mold device and consulting relationship with COSM Medical, donated research product from RION LLC; CA has research funding and a consulting relationship with Bluewind and research funding from NICHD and NIDDK; SV has industry relationships with OsteoCure Therapeutics and ONCO DiSCOVER. All other authors declare no financial or non-financial competing interests.

Additional information

Correspondence and requests for materials should be addressed to Cassandra K. Kisby.